JOC The Journal of Organic Chemistry

Note

pubs.acs.org/joc

An NMR and MD Modeling Insight into Nucleation of 1,2-Alkanediols: Selective Crystallization of Lipase-Catalytically Resolved Enantiomers from the Reaction Mixtures

Omar Parve,[†] Indrek Reile,[‡] Jaan Parve,[§] Sergo Kasvandik,[§] Marina Kudrjašova,[†] Sven Tamp,[†] Andrus Metsala,[†] Ly Villo,*[,†] Tõnis Pehk,[‡] Jüri Jarvet,[‡] and Lauri Vares[§]

[†]Department of Chemistry, Tallinn University of Technology, Ehitajate tee 5, 19086 Tallinn, Estonia

[‡]National Institute of Chemical Physics and Biophysics, Akadeemia tee 23, 12618 Tallinn, Estonia

[§]Institute of Technology, University of Tartu, Nooruse 1, 50411 Tartu, Estonia

Supporting Information

ABSTRACT: The work on developing a scalable lipase-catalytic method for the kinetic resolution of long-chain 1,2-alkanediols, complemented by crystallization of the pure enantiomers from the reaction mixtures, offered the possibility of a more detailed study of the aggregation of such diols. MD modeling, mass spectrometry, ^{1}H NMR, and DOSY studies provided a novel insight into the nucleation process. An efficient protocol for stereo- and chemoselective crystallization of (*S*)-**1**,2-dodecanediol and related compounds from the crude bioconversion mixtures was developed.

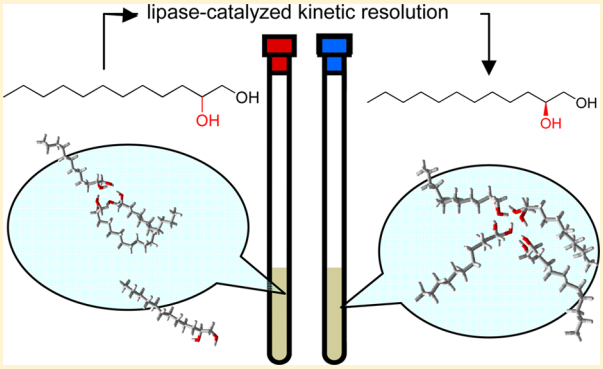

Enantiomers of 1,2-alkanediols **1** and **2** (Scheme 1) and related tetrols are valuable chiral building blocks for synthesis of biologically active compounds.[1] Alcohols of this type have been prepared by hydrolytic kinetic resolution of terminal epoxides.[2−4] Asymmetric dihydroxylation of olefins[5] and diboration/oxidation of olefins and alkynes[6] have also been used. A regiodivergent chemical catalytic stereoresolution[7] as well as an enzymatic asymmetric oxidation of β-hydroxy ketones[8] afforded enantiomeric 1,2-alkanediols with regioselectively protected *sec*-OH groups. In lipase-catalytic resolutions, enantiomeric 1,2-alkanediols with protected primary OH groups have been gained.[9,10] Enzymatic methods for the preparation of enantiopure 1,2-alkanediols[11−14] based on lipase-catalyzed reactions or on epoxide cleavage by epoxide hydrolases[15] have previously been proposed.

Scheme 1. Separation of (*S*)-1,2-Alkanediols from Racemic Mixtures: (a) Chemical Butyrylation; (b) Lipase-Catalyzed Methanolysis; (c) Crystallization of the Pure Enantiomer from the Crude Product

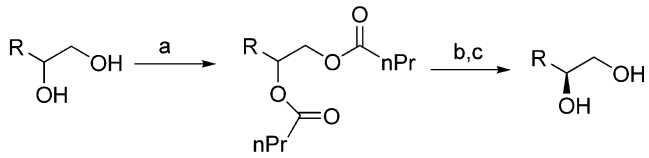

1: R=C_6H_{13}
2: R=$C_{10}H_{21}$

3: R=C_6H_{13}
4: R=$C_{10}H_{21}$

(*S*)-1
(*S*)-2

Despite the above-mentioned results, the availability of long-chain enantiomeric 1,2-alkanediols has been deemed insufficient. The objective of our work was to develop a scalable stereoselective lipase-catalytic method for the separation of pure stereoisomers without using chromatography.[16] Molecular dynamics (MD) modeling and ^{1}H NMR and diffusion-ordered NMR spectroscopy (DOSY) studies of the aggregation of enantiomeric versus racemic 1,2-alkanediols were carried out with the aim of developing a method for stereo- and chemoselective crystallization of an alcohol enantiomer from the reaction mixture. The other part of the work involved screening of the reagents and conditions for the lipase-catalyzed kinetic resolution. Herein we present results that are of general significance and provide (1) a novel insight into the nucleation process based on analytical data and MD modeling and (2) a protocol for lipase-catalyzed stereoselective preparation and prompt selective crystallization of pure 1,2-alkanediol enantiomers from the crude products. To provide a better outline of the goal of the nucleation studies, the following short description of the developed separation protocol is given.

Screening of the conditions and reagents for the biotransformations resulted in a protocol based on methanol-

Received: October 4, 2013
Published: November 7, 2013

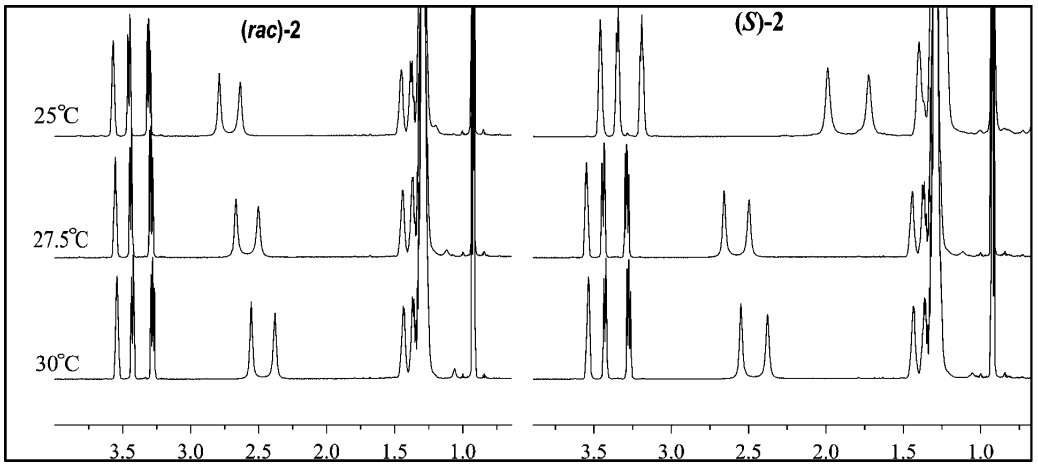

Figure 1. ^{1}H NMR spectra of *rac*-**2** and (*S*)-**2** recorded in C_6D_6 (0.1 M) at 25, 27.5, and 30 °C.

ysis of an ester catalyzed by *Candida antarctica* lipase B (CalB) (Scheme 1).[14] Racemic diols **1** and **2** were esterified, and the resulting butyric esters **3** and **4**, respectively, were allowed to undergo enzymatic methanolysis without previous purification. The target diols (*S*)-**1** and (*S*)-**2** (*er* > 98/2 in the crude product) were separable from the crude methanolysis products [usually consisting of 40−45% target (*S*)-**1** or (*S*)-**2**, 50−55% (*R*)-2-monobutyrate, and 5−10% starting bisbutyrate **3** or **4**] in high chemical and stereochemical purity by a single crystallization. For instance, the crude product of (*S*)-**2** obtained starting from 1 g of *rac*-**2** was dissolved in $CHCl_3$ (2 mL), and resulting solution was cooled by stirring shortly on an ice bath. As a result, (*S*)-**2** was crystallized from the mixture and gained in up to 26% yield with a very good *er* (>99.9/0.1); (*S*)-**1** was crystallized from the crude product in $CHCl_3$ by storage at −15 °C. All of the crystallized products showed higher *er* than the rest of the substance remaining in the mother liquor. Furthermore, when as high a concentration as 0.5 M for substrate **4** was used in enzymatic methanolysis in CH_3CN/CH_3OH (96/4), a significant in situ crystallization of liberated (*S*)-**2** was observed during incubation. In order to allow direct separation of the crystalline product, immobilized CalB (Novozym 435) was used in removable paper bags. No negative influence on the reaction rate nor conversion was observed when the enzyme was used in such a freely permeable "CalB bag" with magnetic stirring.

The crystallization studies started from the ^{1}H NMR spectra of (*S*)-**2** recorded in $CDCl_3$ and C_6D_6 (both 0.1 M) at 25 °C, which were found to differ from each other and from the corresponding spectra of *rac*-**2** (Figure 1). An ^{1}H NMR spectrum of a nonracemic mixture of enantiomers of diol **2** was recorded in this study, but no split signals were observed. This confirmed that the difference between the NMR spectra of (*S*)-**2** and *rac*-**2** cannot be explained by the formation of diastereomeric dimer aggregates.[17] A test of the influence of temperature (Figure 1) revealed the probable relation of the above spectral effects to a phase transition. The aggregation observed in liquid phase could be considered as the beginning of the nucleation of (*S*)-**2** leading smoothly to crystallite formation. The nucleation processes of (*S*)-**2** versus *rac*-**2** were studied in detail by DOSY, MD simulations, and Orbitrap MS because (*S*)-**2** is an important chiral building block for the synthesis of acetogenin analogues to be performed in our laboratory.

DOSY methods yield data that can be used to extract information about molecular dimensions, aggregation, and molecular mass.[18,19] In this work, ^{1}H NMR and DOSY were used to provide insight into the solution-state structures of *rac*-**2** and (*S*)-**2**. C_6D_6 was chosen for this work because it allows anisotropic solvation [section 4 in the Supporting Information (SI)] and is a more viscous medium than $CDCl_3$.

At 30 and 27.5 °C, the ^{1}H NMR spectra (Figure 1) as well as the DOSY spectra of (*S*)-**2** (Figure 2) and *rac*-**2** (see the SI)

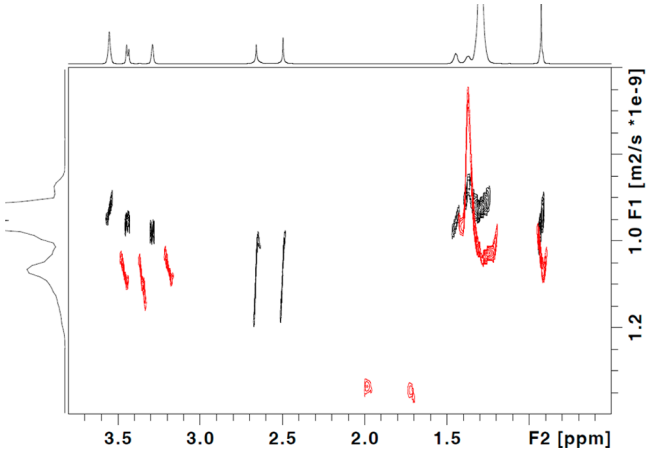

Figure 2. DOSY spectra of (*S*)-**2** recorded in C_6D_6 (0.1 M) at 27.5 °C (black) and 25 °C (red).

overlap, displaying identical chemical shifts and diffusion coefficients (*D*) (Table 1). The latter were found to be 25% lower than would be expected for a compound with

Table 1. Diffusion Coefficients (*D*) Measured for Racemic and Enantiopure Diols 2 in C_6D_6 at Different Temperatures

T (°C)	compd	$D \pm SD^a$ (10^{-9} m^2 s^{-1})
30	*rac*-**2**	1.00 ± 0.02
	(*S*)-**2**	1.01 ± 0.0.02
27.5	*rac*-**2**	0.94 ± 0.02
	(*S*)-**2**	0.94 ± 0.02
25	*rac*-**2**	0.88 ± 0.02
	(*S*)-**2**	1.03 ± 0.04

[a]Average *D* values and standard deviations of three runs are presented.

dx.doi.org/10.1021/jo402189e | J. Org. Chem. 2013, 78, 12795−12801

dodecanediol's molecular weight (MW).[20] A calibration curve of *D* vs MW was constructed using linear hydrocarbons of similar shape (see Figure 6),[21] from which was obtained an apparent MW of 301 g/mol for **2**, which agrees with the MW estimate of 317 g/mol calculated according to Evans.[20] These values are 1.5 times larger than the MW of compound **2** itself (202 g/mol), suggesting that molecules in solution are bound into H-bonded clusters at the above temperatures. In Orbitrap MS (see the SI), more than two-thirds of the material was detected as dimer aggregates for diol **2** samples, which is in accordance with the DOSY results describing the prenucleation state. A low content of trimer aggregates was detected by MS only for *rac*-**1**. The apparent noninteger MW value of 1.5 units of **2** determined from the *D* value is caused by exchange of bound molecules, which can also explain the above negative result regarding NMR registration of diastereomeric aggregates. The protons of hydroxyl groups displayed higher *D* values than the rest of the molecule, an effect due to the exchange of OH protons with those of the residual water, which is known to influence *D* for labile protons.[22]

Decreasing the temperature to 25 °C caused changes in the ^{1}H NMR (Figure 1) and DOSY (Figure 2) spectra of (*S*)-**2** and also in the DOSY spectrum of *rac*-**2** (see the SI). In the ^{1}H spectrum, extensive upfield shifts of the signals corresponding to the carbinyl and OH protons were observed. Differences in the multiplicities of the signals of H2 and H1 were also observed depending on the medium and on the stereochemical composition of the analyte (see Figure 4). A transition from fast to slow exchange of OH protons was accomplished for (*S*)-**2** in C_6D_6 and in $CDCl_3$ as the temperature decreased from 27.5 to 25 °C, as would be concluded from the appearance of spin−spin coupling between CH and attached OH group hydrogen atoms. This was observed for (*S*)-**2** and not for racemic samples, proving that the temperature change did not directly influence the proton exchange but rather than the proton exchange was slowed down by the formation of H-bonded aggregates of (*S*)-**2** molecules.

Inspection of the DOSY spectrum of *rac*-**2** at 25 °C (see the SI) also revealed the beginning of the formation of aggregates by the signals at 1.3−1.4 ppm. This, however, resulted in the formation of smaller aggregates (as judged by comparison of *D* values; see the SI) that are unable to influence the rate of OH proton exchange.

Unexpectedly, the diffusion of (*S*)-**2** at 25 °C was faster than that at 27.5 °C (Figure 2 and Table 1), while that of *rac*-**2** kept slowing down with decreasing temperature. This could be explained by the onset of a phase transition of (*S*)-**2** between 27.5 and 25 °C. As nucleation and crystallite formation begins, the solution concentration of (*S*)-**2** decreases, allowing the solubilized molecules to diffuse faster.[23] This was confirmed by the concurrent 2.5-fold decrease in the signal-to-noise ratio and 2-fold decrease in the peak integrals compared with the residual solvent peak. As part of the material leaves the solution by crystallite formation, it ceases to contribute to the ^{1}H signal. At lower concentrations, the H-bonding between solubilized molecules becomes less probable, allowing a higher rate of self-diffusion.[24]

In the 25 °C DOSY spectrum of (*S*)-**2** (Figure 2), the curve between 1.3 and 1.4 ppm appears to be due to the presence of slower-diffusing aggregates. One of them has a distinct peak at 1.35 ppm in the ^{1}H NMR spectrum of (*S*)-**2** (Figure 3). This could be resolved well enough to be fitted for monoexponential diffusional attenuation, which yielded $D = 2.72 \pm 0.02 \times 10^{-10}$ m^2 s^{-1}, indicating a 3.8-fold decrease in *D*. Considering that for linear molecules doubling of the MW causes *D* to decrease by 40%,[25] we can assume that this peak corresponds to an octamer or larger aggregate representing a metastable state in the phase transition. This DOSY evidence proves that the unexpected effects observed by decreasing the temperature from 27.5 to 25 °C occurred as a result of the nucleation of (*S*)-**2**.

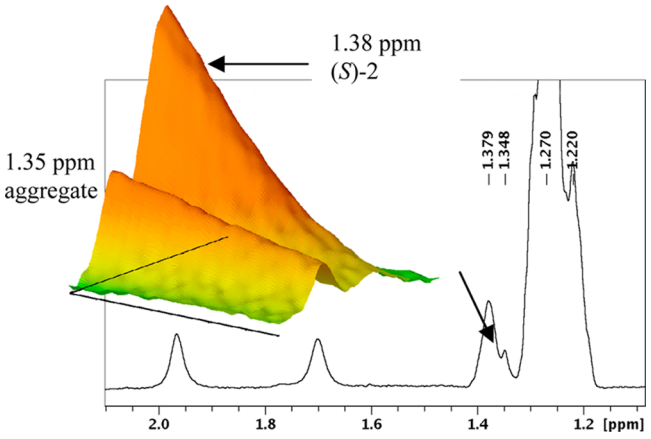

Figure 3. Fragment of the ^{1}H NMR spectrum of (*S*)-**2** in C_6D_6 at 25 °C and (inset) surface plot showing the diffusion decay of dissolved (*S*)-**2** (1.38 ppm) and the slow-diffusing aggregate (1.35 ppm). The emerging auxiliary peaks at 1.35 and 1.22 ppm should be noted.

MD simulations were performed on molecular systems included in a solvent box (in C_6H_6 or in $CHCl_3$); the MD results are presented in Table 2 and Figure 5 (also see the SI). The following five conclusions from the MD simulation results can be drawn: (1) (*S*)-**2** in $CHCl_3$ at 25 °C can form a stable tetramer aggregate (Figure 5a) that could be a starting step in the nucleation. (2) Homochiral aggregation of diol enantiomers is more sustainable than heterochiral aggregation of racemic samples, as more tetramers are formed in the former case (Table 2). (3) The average energy of the 10 preferable systems found for *rac*-**1** (all involving a trimer) is lower than that found for (*S*)-**1**. This apparently irregular theoretical result is in accordance with an unexpected experimental result: in Orbitrap MS, trimers were detected only for *rac*-**1**. (4) Benzene, compared with chloroform, is less suitable for the aggregation of diol molecules because of the limited formation of H-bonds (Table 2). (5) The differences in the multiplicities of the signals of H2 and H1 of (*S*)-**2** depending on the medium (Figure 4a,c), when compared with the corresponding geometries of the more probable molecular aggregates in these media (Figure 5a,c), suggest that the H-bonding pattern of the aggregates can determine the nature of the spin−spin coupling between the CH hydrogen and the hydrogen of the attached OH group.

In sum, several ^{1}H and DOSY spectral indications together with MD simulation results have provided a novel insight into the nucleation process. A simple protocol for stereo- and chemoselective crystallization of (*S*)-1,2-dodecanediol and enantiomers of related compounds from complex reaction mixtures was developed. The in situ-crystallized enantiomeric product can be separated from the reaction mixture without halting the biotransformation

■ EXPERIMENTAL SECTION

General Experimental Methodology for Diffusion-Ordered NMR Spectroscopy. Diffusion NMR experiments were run in standard 5 mm NMR tubes at different temperatures (25, 27.5, and 30

dx.doi.org/10.1021/jo402189e | J. Org. Chem. 2013, 78, 12795−12801

Table 2. Results of MD Simulations

run	molecular system of four molecules	medium	T (°C)	total no. of molecular aggregates in 3000 MD trajectory snapshots: dimer	trimer	tetramer	ratio of tetramers to trimers	average energy (kcal/mol)[a]	ΔE (kcal/mol)[b]
1	(*S*)-**2**	$CHCl_3$	25	913	434	372	0.86	377.8	
2	*rac*-**2**	$CHCl_3$	25	988	373	91	0.24	409.4	+31.6
3	(*S*)-**2**	C_6H_6	25	976	359	0	0	392.9	
4	*rac*-**2**	C_6H_6	25	1410	220	4	0.02	406.6	+13.7
5	(*S*)-**1**	$CHCl_3$	25	1834	319	109	0.34	274.8	
6	*rac*-**1**	$CHCl_3$	25	945	245	0	0	269.9	−4.9
7	(*S*)-**2**	C_6H_6	30	1084	163	83	0.51	392.2	
8	*rac*-**2**	C_6H_6	30	1531	98	49	0.50	402.9	+10.7

[a]Energies based on MD trajectory snapshots. The systems were not additionally minimized; average energies of 10 energetically preferable molecular systems are presented. [b]$\Delta E = E_{rac} - E_{(S)}$.

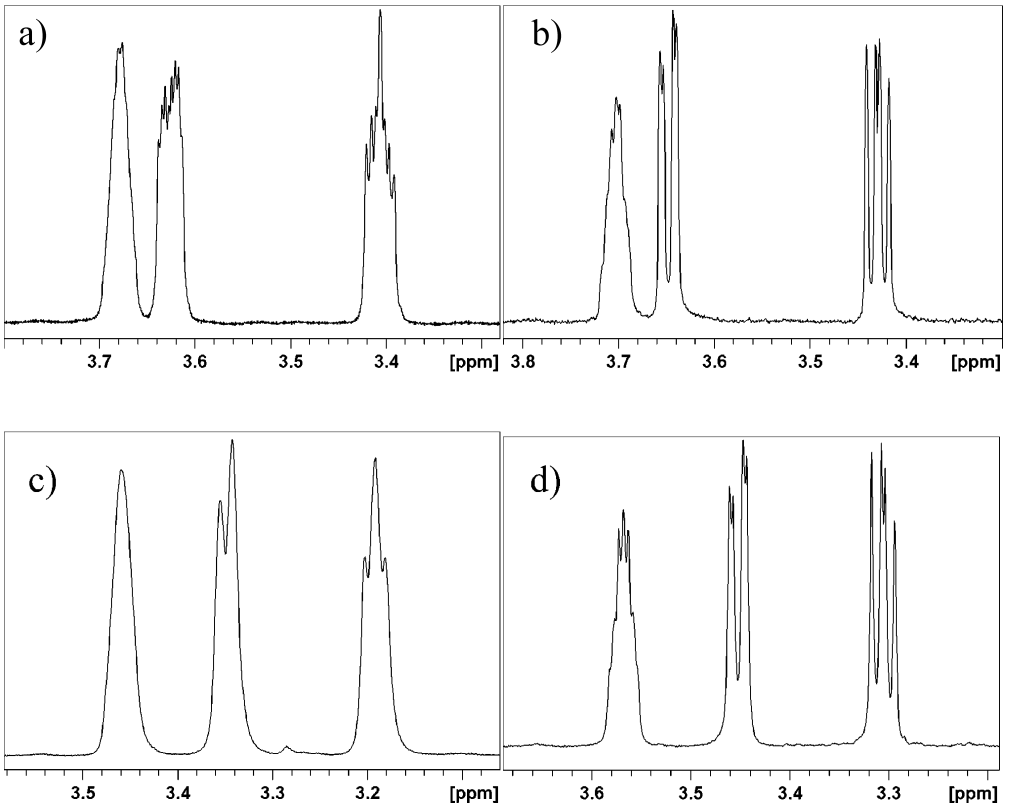

Figure 4. Signals of hydrogen atoms H2, H1, and H1 (left to right) in the NMR spectra of enantiopure vs racemic diol **2** (0.1 M) recorded on an 800 MHz instrument at 25 °C in different media: (a) (*S*)-**2** in $CDCl_3$; (b) *rac*-**2** in $CDCl_3$; (c) (*S*)-**2** in C_6D_6; (d) *rac*-**2** in C_6D_6. The original spectra are presented in the SI.

°C). The probe was allowed to thermally stabilize after temperature change. A further 30 min of stabilization was allowed for each sample after its insertion into the magnet and before acquisition to avoid temperature gradients in the sample. All of the samples were prepared by dissolving an appropriate amount of pure crystalline substance in $CDCl_3$ or C_6D_6. Experiments were run on an 800 MHz spectrometer equipped with a PADUL probe with a *z*-axis gradient coil. All experiments were run without spinning the sample. The standard convection-compensated pulse program dstebpgp3s was used with bipolar rectangular gradients of 1 ms and a diffusion time of 150 ms. The gradient was changed linearly in 32 steps from 5% to 95% of the gradient strength, and all rows were phase- and baseline-corrected. Diffusion coefficients (D) were obtained with the TopSpin T1/T2 module. D values were measured for 0.1 M solutions of 1-octene, 1-tetradecene, and eicosane and used to construct a calibration curve[21] (Figure 6) for evaluating the MW of **2**.

Direct-Infusion ESI-FTMS Experiments by Orbitrap Mass Spectrometry. All crystalline samples were dissolved (10 and 100 mM) in $CHCl_3$. The dissolved samples were infused into an LTQ Orbitrap mass spectrometer using a medium borosilicate nano-ESI offline emitter. The ionization was performed at room temperature, and the spray voltage and tube lens were set to 1.8 kV and 140 V, respectively. Positive mode spectra over the range m/z 120−1000 were collected and averaged at a resolution setting of 100 000 at m/z 400. The AGC target for FTMS analysis was 1×10^6 ions. The ion transfer capillary was kept at either 180 or 50 °C, but it was noted that this did not affect the measured spectra.

Computational Methodology for Molecular Dynamics Simulations. The systems consisting of four diol molecules with the *S* configuration were considered as pure enantiomers, and two

dx.doi.org/10.1021/jo402189e | J. Org. Chem. 2013, 78, 12795−12801

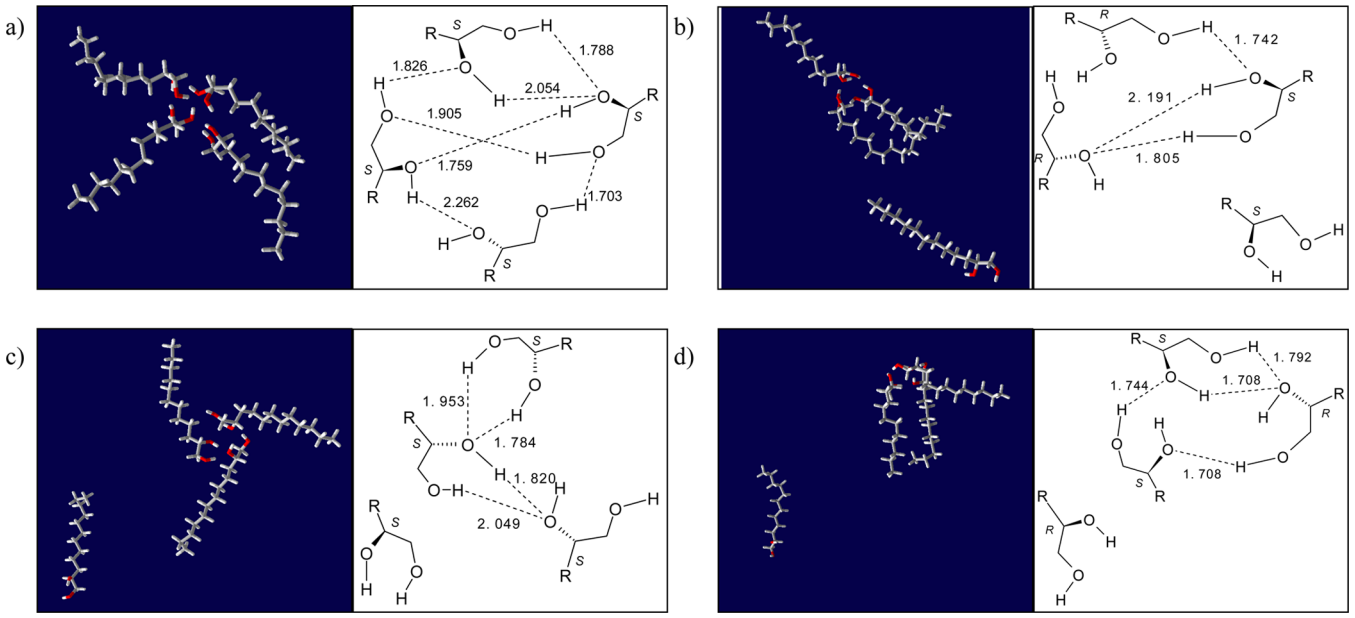

Figure 5. Models and schemes of the most probable molecular aggregates identified from the MD simulation trajectories (25 °C): (a) (*S*)-**2** in $CHCl_3$; (b) *rac*-**2** in $CHCl_3$; (c) (*S*)-**2** in C_6H_6; (d) *rac*-**2** in C_6H_6.

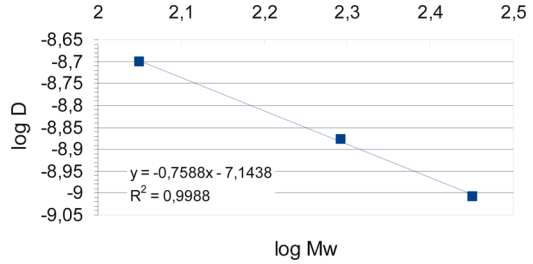

Figure 6. Calibration curve of diffusion coefficient (D) vs MW constructed using standard 0.1 M solutions of 1-octene, 1-tetradecene, and eicosane in C_6D_6.

molecules with *S* configuration together with two molecules with *R* configuration were investigated as racemates. Molecular mechanics and MD calculations were performed with the program YASARA.[26] The initial molecular systems for calculation were prepared with the program VEGA.[27] Thereafter, a rectangular simulation cell around all of the diol molecules with dimensions of 50 Å × 50 Å × 50 Å was created. In order to mimic the influence of solvent during MD runs, the simulation cell was "filled" with molecules of the desired solvent in such a way that the solvent density fulfilled the following density values: 1.48 g/mL for chloroform and 0.88 g/mL for benzene. In such a way, 838 benzene and 975 chloroform molecules appeared within the corresponding simulation cells. The systems prepared as described above were transferred into the program YASARA. The pre-MD-simulation steps were performed as follows: A three-stage structure relaxation and energy minimization procedure for the diol systems was performed. In the first stage, only the diol molecules were minimized without solvent. In the second stage, the solvent moiety was minimized only. In the third stage, the energy of the entire system was minimized. When solvated in such a way, the systems under study were used in MD simulations with a time interval of 30 ns. The force field used for MD simulations was AMBER99[28] with a cutoff value of 7.86 Å for the van der Waals forces; for the long-range electrostatics, the particle-mesh Ewald (PME) approach[29] was used. The simulation was run under periodic boundary conditions at 298 K and 1.0 atm unless otherwise mentioned. Multiple time steps were used: 1.25 fs for intramolecular forces and 2 × 1.25 fs for intermolecular forces. After each 10 ps time interval, all of the coordinates of the molecular systems were saved as a snapshot frame. MD simulation results were analyzed further with the help of YASARA; the trajectory analysis was performed with the VMD molecular visualization and analysis package.[30] The cluster behavior (tetrameric, trimeric, and dimeric aggregates of diol molecules) was analyzed with the help of our original software.

Lipase-Catalyzed Kinetic Resolution of Stereoisomers. *General Experimental Methodology.* ^1H and ^{13}C NMR spectra were recorded in $CDCl_3$ and C_6D_6 solutions on 800 and 400 MHz spectrometers. All signals were referenced relative to solvent signals. 2D FT methods were used for the full assignment of NMR spectra. Column chromatography was performed on Merck silica gel 60 (230–400 mesh). TLC was performed using DC-Alufolien Kieselgel 60 F_{254} (Merck) silica gel plates and analyzed by staining upon heating with anisaldehyde solution (3 mL of anisaldehyde and 10 mL of conc. H_2SO_4 in 90 mL of EtOH). Racemic 1,2-octanediol and 1,2-dodecanediol were used in lipase-catalyzed kinetic resolution without additional purification.

Separation of (S)-1,2-Dodecanediol from a Racemic Mixture. Racemic 1,2-dodecanediol (*rac*-**2**) (1.01 g, 5 mmol) was dissolved in pyridine (4 mL) on slight heating; petroleum ether (12 mL) was added, and the mixture was shaken until homogenized. Butyryl chloride (1.28 g, 1.25 mL, 12 mmol, 2.4 equiv) was added dropwise with efficient magnetic stirring. The mixture was stirred at RT for 15 min. When the reaction was complete by TLC, methanol (0.5 mL, 12.3 mmol) was added to the reaction mixture, and stirring was allowed to continue for an additional 10 min. Petroleum ether (40 mL) was added, followed by 15 mL of 10% $NaHCO_3/H_2O$ solution. After the neutralization had completed, the water layer was separated, and the organic solution was washed with brine (2 × 15 mL). The solution was dried over anhydrous $MgSO_4$, filtered, concentrated, and used in the subsequent enzymatic methanolysis step without purification. The crude bisbutyrate *rac*-**4** was dissolved in acetonitrile (9.6 mL) with magnetic stirring, and methanol (0.4 mL) was added. Novozym 435 (immobilized *C. antarctica* lipase B, 0.5 g) was introduced in a removable paper bag and allowed to incubate for 48 h at RT with magnetic stirring. The paper bag containing the enzyme was removed (it was washed with EtOAc, and the washings were added to the mother liquor), and crystalline (*S*)-**2** was filtered off (105 mg, 10.4% yield). The product was 1-tosylated, and an *er* of 99.9/0.1 was determined using chiral-stationary-phase HPLC (the chromatograms are presented in the SI). The homogeneity and identity of the product were verified by NMR analysis [^{13}C NMR spectra of *rac*-**2** vs (*S*)-**2** are presented in section 4 in the SI).

dx.doi.org/10.1021/jo402189e | J. Org. Chem. 2013, 78, 12795–12801

The mother liquor of the crude methanolysis product was concentrated, and 2 mL of $CHCl_3$ was added. The material was dissolved by slight heating, and the solution was shortly (for 5 min) cooled with magnetic stirring on an ice bath. As a result, an additional portion of (*S*)-**2** crystallized from the crude product and was isolated as described above (155 mg; total 260 mg, ∼26% yield). The *er* of the additional portion of the product as well as its spectral characteristics were identical to those of the former, spontaneously crystallized portion.

*rac-1,2-Dodecanediol Bisbutyrate (**4**).* The synthesis was performed following the protocol described above as a part of the integrated procedure for the separation of (*S*)-1,2-dodecanediol from the racemic mixture. Starting from 1.01 g (5 mmol) of *rac*-**2**, 1.641 g (95.8% yield) of the target bisbutyrate was obtained after flash chromatography over silica gel. ^{1}H NMR (400 MHz, $CDCl_3$): δ 5.02 (1H, m, H-2), 4.16 (1H, dd, J = 3.4 and 11.9 Hz, H-1), 3.96 (1H, dd, J = 6.8 and 11.9 Hz, H-1), 2.22 (4H, t, J = 7.4 Hz, Bu-2), 1.58 (4H, m, Bu-3), 1.49 (2H, m, H-3), 1.20 (16H, m, H4−H11), 0.88 and 0.87 (2 × 3H, t, J = 7.4 Hz, Bu-4), 0.81 (3H, t, J = 7.0 Hz, H-12). ^{13}C NMR (101 MHz, $CDCl_3$): δ 173.4 and 173.2 (Bu-1), 71.3 (C-2), 64.9 (C-1), 36.3 and 36.0 (Bu-2), 31.9 (C-10), 30.8 (C-3), 29.6, 29.5, 29.4, 29.4, 29.3 (C-5−C-9), 25.1 (C-4), 22.7 (C-11), 18.5 and 18.4 (Bu-3), 14.1 (C-12), 13.6 and 13.6 (Bu-4). MS (m/z): 343, 255, 241, 211, 201, 184, 173, 166, 153, 144, 142, 138, 124, 110, 97, 82, 71. IR (neat, cm^{-1}): 1090, 1176, 1253, 1381, 1461, 1742, 2856, 2928. Anal. Calcd for $C_{20}H_{38}O_4$ (342.58): C, 70.12; H, 11.20. Found: C, 70.16; H, 11.23. TLC: R_f = 0.39 (EtOAc/petroleum ether 0.4/10). Flash chromatography eluent: EtOAc/petroleum ether 0.15/10.

*(S)-**2**.*[31] $[\alpha]_D^{20}$ −14 (c 1.0, EtOH). IR (KBr; cm^{-1}): 530, 582, 662, 720, 838, 871, 972, 992, 1006, 1032, 1053, 1073, 1105, 1135, 1311, 1335, 1470, 2850, 2919, 3240, 3323, 3478. Anal. Calcd for $C_{12}H_{26}O_2$ (202.38): C, 71.21; H, 12.98. Found: C, 71.20; H, 13.01. TLC: R_f = 0.14 (6/10 EtOAc/petroleum ether). Flash chromatography eluent: 1/2 EtOAc/petroleum ether. Mp = 68−70 °C.

Separation of (S)-1,2-Octanediol from a Racemic Mixture. Racemic 1,2-octanediol (*rac*-**1**) (0.730 g, 5 mmol) was dissolved in pyridine (6 mL, ∼6 equiv) on slight heating; petroleum ether (10 mL) was added, and the mixture was shaken until homogenized. Butyryl chloride (1.28 g, 1.25 mL, 12 mmol, 2.4 equiv) was added dropwise with efficient magnetic stirring. The mixture was stirred at RT for 15 min. When conversion was estimated to be complete by TLC, methanol (0.5 mL, 12.3 mL) was added to the reaction mixture, and stirring was continued for an additional 10 min. Petroleum ether (40 mL) was added, followed by 15 mL of 10% $NaHCO_3/H_2O$ solution. After the neutralization had completed, the water layer was separated, and the organic solution was washed with brine (2 × 15 mL). The solution was dried over anhydrous $MgSO_4$, filtered, evaporated, and used in the subsequent enzymatic methanolysis step without purification. The crude bisbutyrate *rac*-**3** was dissolved in acetonitrile (19.2 mL) with magnetic stirring, and methanol (0.8 mL) was added. Novozym 435 (0.5 g) was introduced and allowed to incubate (on shaking) at RT during 48 h. The conversion of the second step was estimated by TLC to be 40−50%. The enzyme was filtered off, and the crude product was concentrated and dissolved by heating in $CHCl_3$ (2 mL). The solution was stored at −15 °C for 14 h. Crystalline (*S*)-1,2-octanediol was filtered off and washed with cooled (5 °C) petroleum ether, affording 139 mg (19% yield) of crystalline product. The product was 1-tosylated, and an *er* 99.9/0.1 was determined by chiral-stationary-phase HPLC (the chromatograms are presented in the SI). The homogeneity and identity of the product were verified by NMR analysis.

*rac-1,2-Octanediol Bisbutyrate [(rac)-**3**].* The synthesis was performed following the protocol described above as a part of the integrated procedure for the separation of (*S*)-1,2-octanediol from the racemic mixture. Starting from 0.730 g (5 mmol) of *rac*-**1**, 1.392 g (97.2% yield) of the target bisbutyrate **3** was obtained after flash chromatography over silica gel. ^{1}H NMR (400 MHz, $CDCl_3$): δ 5.03 (1H, m, H-2), 4.16 (1H, dd, J = 3.4 and 11.7 Hz, H-1), 3.96 (1H, dd, J = 6.8 and 11.7 Hz, H-1), 2.22 (4H, t, J = 7.5 Hz, Bu-2), 1.58 (4H, m, Bu-3), 1.49 (2H, m, H-3), 1.22 (8H, m, H4−H7), 0.88 and 0.87 (2 × 3H, t, J = 7.4 Hz, Bu-4), 0.81 (3H, t, J = 7.0 Hz, H-8). ^{13}C NMR (101 MHz, $CDCl_3$): δ 173.3 and 173.1 (Bu-1), 71.3 (C-2), 64.9 (C-1), 36.3 and 36.0 (Bu-2), 31.6 (C-7), 30.8 (C-3), 29.0 (C-5), 25.0 (C-4), 22.5 (C-7), 18.5 and 18.3 (Bu-3), 14.0 (C-8), 13.60 and 13.58 (Bu-4). MS (m/z): 288, 287, 199, 185, 173, 144, 142, 129, 114, 111, 103, 100, 97, 95, 89, 82, 71, 69, 43. IR (neat, cm^{-1}): 1096, 1175, 1254, 1380, 1462, 1741, 2875, 2962. Anal. Calcd for $C_{16}H_{30}O_4$ (286.46): C, 67.08; H, 10.58. Found: C, 67.01; H, 10.62. TLC: R_f = 0.35 (EtOAc/petroleum ether 0.4/10). Flash chromatography eluent: EtOAc/petroleum ether 0.2/10.

*(S)-**1**.*[32] $[\alpha]_D^{20}$ −14.4 (c 1.0, MeOH); mp = 43−45 °C. Original NMR spectra are shown in section 6.5 in the SI. IR (KBr, cm^{-1}): 438, 491, 537, 581, 654, 723, 861, 881, 988, 1017, 1044, 1092, 1136, 1215, 1251, 1334, 1469, 2857, 2929, 3318, 3477. Anal. Calcd for $C_8H_{18}O_2$ (146.26): C, 65.69; H, 12.43. Found: C, 65.63; H, 12.38. TLC: R_f = 0.08 (eluent: 6/10 EtOAc/petroleum ether). Flash chromatography eluent: 7/10 EtOAc/petroleum ether.

Analysis of the (S)-1,2-Alkanediols in the Form of 1-Tosylates[33] Using HPLC over a Chiral Stationary Phase. *Synthesis of the 1-Tosylate of (S)-1,2-Octanediol.*[33] (*S*)-1,2-Octanediol (68 mg, 0.463 mmol) was dissolved in dichloromethane (5 mL), and triethylamine (52 mg, 72 μL, 0.51 mmol, 1.1 equiv) was added with stirring at RT. Tosyl chloride (97 mg, 0.51 mmol, 1.1 equiv) was added, followed by a catalytic amount of dibutyltin oxide (5 mg, 0.02 mmol), and stirring of the mixture was continued at RT for 16 h. Subsequently, EtOAc (60 mL) was added, and the resulting solution was washed with $NaHCO_3$ and brine, dried over anhydrous Na_2SO_4, filtered, and concentrated. The crude product was purified by chromatography over silica gel to afford the target (*S*)-1-tosyl-1,2-octanediol (108 mg, 77.7% yield).

(S)-1-Tosyl-1,2-octanediol. ^{1}H NMR (400 MHz, $CDCl_3$): δ 7.83 (2H, dm, J = 8.4 Hz, Tos-2,6), 7.38 (2H, dm, J = 8.4 Hz, Tos-3,5), 4,07 (1H, dd, J = 2.8 and 9.9 Hz, H-1), 3.90 (1H, dd, J = 7.2 and 9.9 Hz, H-1), 3.86 (1H, m, H-2), 2.48 (3H, s, Tos-CH_3), 2.12 (1H, bs, 2-OH), 1.43 (3H, m, H-3, H-4), 1.28 (7H, m, H-4, H-5−H-7), 0.89 (3H, t, J = 2 × 7.1 Hz, H-8). ^{13}C NMR (101 MHz, $CDCl_3$): δ 145.0 (Tos-4), 132.7 (Tos-1), 129.9 (Tos-3,5), 127.9 (Tos-2,6), 74.0 (C-1), 69.5 (C-2), 32.6 (C-3), 31.6 (C-6), 29.1 (C-5), 25.1 (C-4), 22.5 (C-7), 21.6 (Tos-CH_3), 14.0 (C-8). MS (m/z): 302, 301, 271, 252, 215, 157, 156, 116, 97, 93, 91, 71, 55. Determination of the specific rotation failed; the value was <1.5 (EtOAc). IR (neat, cm^{-1}): 556, 668, 815, 899, 965, 1098, 1177, 1360, 1457, 1599, 2858, 2930, 3535. Anal. Calcd for $C_{15}H_{24}O_4S$ (300.45): C, 59.96; H, 8.07. Found: C, 59.90; H, 8.11. TLC: R_f = 0.27 (EtOAc/petroleum ether 2/10). Flash chromatography eluent: EtOAc/petroleum ether 2/10.

Synthesis of the 1-Tosylate of (S)-1,2-Dodecanediol.[33] (*S*)-1,2-Dodecanediol (110 mg, 0.54 mmol) was dissolved in dichloromethane (5 mL), and triethylamine (60 mg, 83 μL, 0.59 mmol, 1.1 equiv) was added with stirring at RT. Tosyl chloride (112 mg, 0.59 mmol, 1.1 equiv) was added, followed by a catalytic amount of dibutyltin oxide (5 mg; 0.02 mmol), and stirring was continued for 16 h. EtOAc (60 mL) was added, and the solution was washed with $NaHCO_3$ and brine and dried over anhydrous Na_2SO_4. The solution was filtered and concentrated. The crude product was purified by chromatography over silica gel (eluent: 16% EtOAc/petroleum ether) to afford the target (*S*)-1-tosyl-1,2-dodecanediol (143 mg, 74% yield).

*(S)-**1**-Tosyl-1,2-dodecanediol.* ^{1}H NMR (400 MHz, $CDCl_3$): δ 7.83 (2H, dm, J = 8.3 Hz, Tos-2,6), 7.38 (2H, dm, J = 8.3 Hz, Tos-3,5), 4,07 (1H, dd, J = 2.7 and 9.8 Hz, H-1), 3.90 (1H, dd, J = 7.1 and 9.8 Hz, H-1), 3.84 (1H, m, H-2), 2.48 (3H, s, Tos-CH_3), 2.12 (1H, bs, 2-OH), 1.43 (3H, m, H-3, H-4), 1.28 (15H, m, H-4, H-5−H-11), 0.90 (3H, t, J = 2 × 7.1 Hz, H-12). ^{13}C NMR (101 MHz, $CDCl_3$): δ 145.1 (Tos-4), 132.7 (Tos-1), 130.0 (Tos-3,5), 128.0 (Tos-2,6), 74.0 (C-1), 69.5 (C-2), 32.7 (C-3), 31.9 (C-10), 29.59, 29.55, 29.47, 29.45, 29.33 (C-5−C-9), 25.2 (C-4), 22.7 (C-11), 21.7 (Tos-CH_3), 14.1 (C-12). MS (m/z): 357, 339, 326, 308, 263, 243, 215, 171, 157, 156, 140, 125, 111, 97, 92, 83, 71, 57, 55, 43, 41. Determination of the specific rotation failed; the value was <1.0 (EtOAc). IR (KBr, cm^{-1}): 444, 499, 530, 557, 592, 674, 721, 817, 845, 887, 902, 958, 1048, 1107, 1174, 1291, 1308, 1348, 1471, 1597, 2851, 2922, 3549. Anal. Calcd for

dx.doi.org/10.1021/jo402189e | J. Org. Chem. 2013, 78, 12795−12801

$C_{19}H_{32}O_4S$ (356.57): C, 64.00; H, 9.06. Found: C, 63.96; H, 9.04. TLC: R_f = 0.34 (EtOAc/petroleum ether 2/10). Flash chromatography eluent: 1.2/10 EtOAc/petroleum ether.

HPLC Determination of Enantiomeric Ratios. HPLC determination of the enantiomeric ratios of (*S*)-**1** and (*S*)-**2** (as the corresponding 1-tosylates) was performed using an IA column (Daicel Chiralpak IA; 0.46 cm × 25 cm); eluent, 10/90 iPrOH/*n*-hexane; flow rate, 1.0 mL/min; detection, UV 254 nm. The retention times of the 1-tosylates corresponding to the following compounds were 10.33 min for (*R*)-**1**, 12.50 min for (*S*)-**1**, 8.69 min for (*R*)-**2**, and 10.50 min for (*S*)-**2**.

■ ASSOCIATED CONTENT

Supporting Information

Orbitrap MS experimental data; MD simulation data; copies of DOSY, ^{1}H, and ^{13}C NMR spectra; and HPLC chromatograms. This material is available free of charge via the Internet at http://pubs.acs.org.

■ AUTHOR INFORMATION

Corresponding Author

*E-mail: lee@chemnet.ee.

Notes

The authors declare no competing financial interest.

■ ACKNOWLEDGMENTS

The authors are grateful to the Estonian Ministry of Education and Research (Grants SF0140133s08, SF0690021s09, SF0690034s09, ETF8880, SF0180073s08, SF0140060s12). We thank the Archimedes Foundation (Project 3.2.0501.10-0004). Mass spectrometric analyses were in part supported by the European Regional Development Fund through the Center of Excellence in Chemical Biology.

■ REFERENCES

(1) Challenger, C. A. *Chiral Intermediates*; Wiley: London, 2001.
(2) Tokunaga, M.; Larrow, J. F.; Kakiuchi, F.; Jacobsen, E. N. *Science* **1997**, *277*, 936.
(3) Chow, S.; Kitching, W. *Chem. Commun.* **2001**, 1040.
(4) Bredihhina, J.; Villo, P.; Andersons, K.; Toom, L.; Vares, L. *J. Org. Chem.* **2013**, *78*, 2379.
(5) Kolb, H. C.; Van Nieuwenhze, M. S.; Sharpless, K. B. *Chem. Rev.* **1994**, *94*, 2483.
(6) Lee, Y.; Jang, H.; Hoveyda, A. H. *J. Am. Chem. Soc.* **2009**, *131*, 18234.
(7) Worthy, D.; Sun, X.; Tan, K. L. *J. Am. Chem. Soc.* **2012**, *134*, 7321.
(8) Kirschner, A.; Bornscheuer, U. *Angew. Chem., Int. Ed.* **2006**, *45*, 7004.
(9) Shimada, Y.; Sato, H.; Minowa, S.; Matsumoto, K. *Synlett* **2008**, 367.
(10) Kim, M.-J.; Choi, Y. K. *J. Org. Chem.* **1992**, *57*, 1605.
(11) Poppe, L.; Novák, L.; Kajtár-Peredy, M.; Szántay, C. *Tetrahedron: Asymmetry* **1993**, *4*, 2211.
(12) Santaniello, E.; Casati, S.; Ciuffreda, P.; Gamberoni, L. *Tetrahedron: Asymmetry* **2005**, *16*, 1705.
(13) Kamal, A.; Chouhan, G. *Tetrahedron Lett.* **2004**, *45*, 8801.
(14) Virsu, P.; Liljeblad, A.; Kanerva, A.; Kanerva, L. T. *Tetrahedron: Asymmetry* **2001**, *12*, 2447.
(15) Simeó, Y.; Faber, K. *Tetrahedron: Asymmetry* **2006**, *17*, 402.
(16) Hungerhoff, B.; Sonnenschein, H.; Theil, F. *Angew. Chem., Int. Ed.* **2001**, *40*, 2492.
(17) Williams, T.; Pitcher, R. G.; Bommer, P.; Gutzwiller, J.; Uskoković, M. *J. Am. Chem. Soc.* **1969**, *91*, 1871.
(18) Johnson, C. S. *Prog. Nucl. Magn. Reson. Spectrosc.* **1999**, *34*, 203.
(19) Cohen, Y.; Avram, L.; Frish, L. *Angew. Chem., Int. Ed.* **2005**, *44*, 520.
(20) Evans, R.; Deng, Z.; Rogerson, A. K.; McLachlan, A. S.; Richards, J. J.; Nilsson, M.; Morris, G. A. *Angew. Chem., Int. Ed.* **2013**, *52*, 3199.
(21) Chen, A.; Wu, D.; Johnson, C. S., Jr. *J. Am. Chem. Soc.* **1995**, *117*, 7965.
(22) Cabrita, E. J.; Berger, S. *Magn. Reson. Chem.* **2002**, *40*, 122.
(23) Durand, E.; Clemancey, M.; Lancelin, J.-M.; Verstraete, J.; Espinat, D.; Quoineaud, A.-A. *J. Phys. Chem. C* **2009**, *113*, 16266.
(24) Jang, H. B.; Rho, H. S.; Oh, J. S.; Nam, E. H.; Park, S. E.; Bae, H. Y.; Song, C. E. *Org. Biomol. Chem.* **2010**, *8*, 3918.
(25) Cohen, Y.; Avram, L.; Evan-Salem, T.; Slovak, S.; Shemesh, N.; Frish, L. In *Analytical Methods in Supramolecular Chemistry*, 2nd ed.; Schalley, C. A., Ed.; Wiley-VCH: Weinheim, Germany, 2012; Vol. *1*, Chapter 6, pp 197 ff.
(26) www.yasara.org (accessed Nov 12, 2013).
(27) www.vegazz.net (accessed Nov 12, 2013).
(28) Cornell, W. D.; Cieplak, P.; Bayly, C. I.; Gould, I. R.; Merz, K. M., Jr.; Ferguson, D. M.; Spellmeyer, D. C.; Fox, T.; Caldwell, J. W.; Kollman, P. A. *J. Am. Chem. Soc.* **1995**, *117*, 5179.
(29) Ewald, P. *Ann. Phys.* **1921**, *369*, 253.
(30) http://www.ks.uiuc.edu/Research/vmd/ (accessed Nov 12, 2013).
(31) Zeng, B.-B.; Wu, Y.; Jiang, S.; Yu, Q.; Yao, Z.-J.; Liu, Z.-H.; Li, H.-Y.; Li, Y.; Chen, X.-G.; Wu, Y.-L. *Chem.—Eur. J.* **2003**, *9*, 282.
(32) Chen, L. S.; Mantovani, S. M.; de Oliveira, L. G.; Duarte, M. C. T.; Marsaioli, A. J. *J. Mol. Catal. B: Enzym.* **2008**, *54*, 50.
(33) Martinelli, M. J.; Nayyar, N. K.; Moher, E. D.; Dhokte, U. P.; Pawlak, J. M.; Vaidyanathan, R. *Org. Lett.* **1999**, *1*, 447.